

# Protein geranylgeranyltransferase-I of *Trypanosoma cruzi*<sup>☆</sup>

Kohei Yokoyama<sup>a,\*</sup>, John R. Gillespie<sup>b</sup>, Wesley C. Van Voorhis<sup>b,c</sup>,  
Frederick S. Buckner<sup>b</sup>, Michael H. Gelb<sup>a,d</sup>

<sup>a</sup> Department of Chemistry, University of Washington, Seattle, WA 98195, USA

<sup>b</sup> Departments of Medicine, University of Washington, Seattle, WA 98195, USA

<sup>c</sup> Departments of Pathobiology, University of Washington, Seattle, WA 98195, USA

<sup>d</sup> Departments of Biochemistry, University of Washington, Seattle, WA 98195, USA

Received 3 July 2007; received in revised form 24 September 2007; accepted 26 September 2007

Available online 2 October 2007

## Abstract

Protein geranylgeranyltransferase type I (PGGT-I) and protein farnesyltransferase (PFT) occur in many eukaryotic cells. Both consist of two subunits, the common  $\alpha$  subunit and a distinct  $\beta$  subunit. In the gene database of protozoa *Trypanosoma cruzi*, the causative agent of Chagas' disease, a putative protein that consists of 401 amino acids with ~20% amino acid sequence identity to the PGGT-I  $\beta$  of other species was identified, cloned, and characterized. Multiple sequence alignments show that the *T. cruzi* ortholog contains all three of the zinc-binding residues and several residues uniquely conserved in the  $\beta$  subunit of PGGT-I. Co-expression of this protein and the  $\alpha$  subunit of *T. cruzi* PFT in *Sf9* insect cells yielded a dimeric protein that forms a tight complex selectively with [<sup>3</sup>H]geranylgeranyl pyrophosphate, indicating a key characteristic of a functional PGGT-I. Recombinant *T. cruzi* PGGT-I ortholog showed geranylgeranyltransferase activity with distinct specificity toward the C-terminal CaaX motif of protein substrates compared to that of the mammalian PGGT-I and *T. cruzi* PFT. Most of the CaaX-containing proteins with X = Leu are good substrates of *T. cruzi* PGGT-I, and those with X = Met are substrates for both *T. cruzi* PFT and PGGT-I, whereas unlike mammalian PGGT-I, those with X = Phe are poor substrates for *T. cruzi* PGGT-I. Several candidates for *T. cruzi* PGGT-I or PFT substrates containing the C-terminal CaaX motif are found in the *T. cruzi* gene database. Among five C-terminal peptides of those tested, a peptide of a Ras-like protein ending with CVLL was selectively geranylgeranylated by *T. cruzi* PGGT-I. Other peptides with CTQQ (Tcj2 DNAJ protein), CAVM (TcPRL-1 protein tyrosine phosphatase), CHFM (a small GTPase like protein), and CQLF (TcRho1 GTPase) were specific substrates for *T. cruzi* PFT but not for PGGT-I. The mRNA and protein of the *T. cruzi* PGGT-I  $\beta$  ortholog were detected in three life-cycle stages of *T. cruzi*. Cytosol fractions from trypomastigotes (infectious mammalian stage) and epimastigotes (insect stage) were shown to contain levels of PGGT-I activity that are ~100-fold lower than PFT activity. The CaaX mimetics known as PGGT-I inhibitors show very low potency against *T. cruzi* PGGT-I compared to the mammalian enzyme, suggesting the potential to develop selective inhibitors against the parasite enzyme.

© 2007 Elsevier B.V. All rights reserved.

**Keywords:** Prenylation; Protein geranylgeranyltransferase-I; Protein farnesyltransferase; CaaX motif; *Trypanosoma cruzi*; Chagas' disease

## 1. Introduction

Prenyl modification of proteins with either farnesyl or geranylgeranyl lipid is required for pivotal cellular events in eukaryotic cells including cell proliferation, apoptosis, and membrane trafficking [1,2]. Two distinct enzymes, protein geranylgeranyltransferase-I (PGGT-I) and protein farnesyltransferase (PFT), are thought to occur in most eukaryotic cells that transfer either a geranylgeranyl or a farnesyl group to proteins containing the C-terminal CaaX motif (where C is cysteine, a is usually an aliphatic amino acid, and X is a variety of amino acids). The C-terminal CaaX motif is a major determinant for recognition either by PGGT-I or PFT. Proteins with Leu or Phe at

**Abbreviations:** PGGT-I, protein geranylgeranyltransferase type-I; PFT, protein farnesyltransferase; PGGT-II, protein geranylgeranyltransferase type-II; *T. cruzi*, *Trypanosoma cruzi*; GGPP, geranylgeranyl pyrophosphate; FPP, farnesyl pyrophosphate; *Sf9*, *Spodoptera frugiperda* 9.

<sup>☆</sup> Note: The nucleotide sequence of *Trypanosoma cruzi* PGGT-I  $\beta$  reported in this paper is available in the GenBank database under the accession number EU113181.

\* Corresponding author at: Department of Chemistry, University of Washington, Campus Box 351700, Seattle, WA 98195, USA. Tel.: +1 206 616 4264; fax: +1 206 685 8665.

E-mail address: [kohey@u.washington.edu](mailto:kohey@u.washington.edu) (K. Yokoyama).

the X position are good substrates of PGGT-I, while those with Ser, Glu, Met or a few other residues are preferred substrates of PFT [2,3]. In *in vitro* enzyme assays, several CaaX proteins including those with X = Met such as K-Ras-CVIM also serve as weak substrates of PGGT-I, and in mammalian cells cultured with a PFT inhibitor these proteins are shown to be geranylgeranylated [4]. Although geranylgeranylated and farnesylated forms of some proteins could have different functions, the alternatively modified proteins seem to be functional in cells, which is thought to be one reason that PFT inhibitors are not highly toxic to mammalian cells [4]. Proteins such as H-Ras-CVLS, that are normally farnesylated but not alternatively modified by PGGT-I in cells treated with a PFT inhibitor, may be mainly responsible for the biological responses of PFT inhibition in the cells [4].

Protein prenyltransferases preferentially operate via an ordered mechanism for binding two substrates with the prenyl pyrophosphate substrate binding first [2,5,6]. Mammalian PGGT-I and PFT form a tight complex selectively with their substrates, geranylgeranyl pyrophosphate (GGPP) and farnesyl pyrophosphate (FPP), respectively [7,8]. Structural and mechanistic studies revealed that critical residues involved in substrate binding occur in the  $\beta$  subunits of mammalian PFT and PGGT-I, and that PGGT-I discriminates FPP at the rate-determining product-release step in which GGPP displaces the geranylgeranylated product [9,10].

Most of Rab family GTPases contain the C-terminal sequence CC, CXC or CCXX and are doubly geranylgeranylated by protein geranylgeranyltransferase-II (PGGT-II), which requires a Rab-escort protein for the substrate recognition [2,11]. Several mammalian Rab GTPases that contain the C-terminal CaaX motif are shown to be preferentially modified by protein geranylgeranyltransferase-II as are other Rab family proteins that are doubly geranylgeranylated [12,13]. After prenyl modification, most proteins with the C-terminal CaaX motif including Rab proteins undergo endoproteolytic removal of the last three amino acids “aaX” followed by carboxyl methylation of the exposed prenyl-cysteine by Ras-conversion enzyme 1 (RCE1) and prenylprotein methyltransferase (PPMT or also known as ICMT), respectively [13,14].

PFT has been found in pathogenic protozoan parasites including trypanosomatids (*T. cruzi*, *T. brucei*, and *Leishmania*), the malaria parasite (*Plasmodium falciparum*), and the enteric parasite *Entamoeba histolytica* [15–18]. PGGT-I has recently been found in *E. histolytica* [19]. *T. brucei* and malaria parasites show high sensitivity to inhibition of PFT compared to mammalian cells [20–23]. We previously reported that potent PFT inhibitors are highly effective in blocking growth of malaria parasites and *T. brucei* bloodstream forms, suggesting the opportunity to develop PFT inhibitors as therapeutics for diseases caused by these parasites [22–25]. It is likely that PFT inhibitors are selectively toxic to these protozoan parasites because of absence of PGGT-I or lack of alternative modification of critical farnesylated proteins in the parasites.

Effective PFT inhibitors to block growth of *T. cruzi* amastigotes in mammalian host cells have not been found, although the growth of *T. cruzi* showed significantly more sensitivity to PFT inhibition than the mammalian cells [15]. Two proteins in *T.*

*cruzi*, TcRho1 GTPase [26] and TcPRL-1 protein tyrosine phosphatase [27] have so far been shown to be farnesylated. Here we describe the cloning of a putative PGGT-I  $\beta$  subunit and co-expression of this gene in combination with the *T. cruzi* PFT  $\alpha$  gene to yield a functional PGGT-I. The recombinant enzyme was characterized by specific complex formation with GGPP, and its substrate specificity with respect to the CaaX motif was studied in comparison with those of mammalian PGGT-I and *T. cruzi* PFT. Protein substrate candidates in the parasite cells for *T. cruzi* PGGT-I and PFT are also discussed. The results may provide insights that will help design protein prenyltransferase inhibitors as anti-*T. cruzi* therapeutics.

## 2. Materials and methods

### 2.1. Materials

Recombinant *T. cruzi* PFT and rat PGGT-I were produced in the baculovirus/*Sf9* cell expression system and purified as described [8,16]. H-Ras-CVLL and other protein substrates produced in *Escherichia coli* were obtained as described [8]. Biotinylated peptides were synthesized, and their structures were verified by mass-spectrometry as described [8]. The peptide segment VDWKDDGVFMAERK of the *T. cruzi* PGGT-I  $\beta$  subunit sequence predicted from the cDNA was synthesized and used to raise the polyclonal antibodies in a rabbit (21st Century Biochemicals, Marlboro, MA). [ $^3$ H]Geranylgeranyl pyrophosphate ( $^3$ H]GGPP) and [ $^3$ H]farnesyl pyrophosphate ( $^3$ H]FPP) were purchased from Perkin-Elmer, and unlabeled GGPP and FPP were from BIOMOL. PGGT-I and PFT inhibitors were obtained as generous gifts from the following sources; GGTI-297, FTI-276, GGTI-2154, and GGTI-2151 from Dr. A.D. Hamilton (Yale University), and GGTI-DU40 from Dr. P. J. Casey (Duke University). *T. cruzi* Tulahuen and CL Brener strains are gifts of Dr. S. Reed (Infectious Diseases Research Institute, Seattle, WA).

### 2.2. Cloning of *T. cruzi* PGGT-I $\beta$ subunit and production of the recombinant baculovirus

cDNA was made from *T. cruzi* (CL Brener) epimastigote total RNA using SuperScript II First-Strand Synthesis System (Invitrogen, Carlsbad, CA) according to the manufacturer's instructions. Genomic DNA was eliminated with RNase-free DNase (Ambion, Austin, TX). The putative *T. cruzi* PGGT-I  $\beta$  subunit (Tc00.1047053508817.150) was identified by TblastN in GeneDB [28]. cDNA was sequenced using spliced-leader RACE and oligo-dT RACE to establish the 5'- and 3'-boundaries of the expressed gene [29]. The defined full length ORF (1206 bp) was then amplified from *T. cruzi* genomic DNA using primers 5'-ccgaattcatgccgcatccgtggtg-3' (sense) and 3'-cctctagactacaaagtctctggaagt-5' (antisense) and ligated into pFastBac (GIBCO/Invitrogen). Transposition of the gene into a bacmid in DH10Bac competent cells, and transfection of *Sf9* cells were carried out according to manufacturer's instructions. The baculovirus was subjected to plaque purification and amplified to a final titer of  $2.8 \times 10^8$  plaque-forming units/ml.

### 2.3. Co-expression of the putative *T. cruzi* PGGT-I $\beta$ with *T. cruzi* PFT $\alpha$ and prenyl-pyrophosphate binding assay

A baculovirus carrying the putative *T. cruzi* PGGT-I  $\beta$  gene alone or together with the *T. cruzi* PFT  $\alpha$  virus [16] was used to infect *Sf9* cells in a 12-well plate ( $0.5 \times 10^6$  cells/well) at a multiplicity of infection of 1–2 for each virus. After the monolayer culture was incubated at 27 °C for 3 days, cells were collected, washed once with phosphate buffered saline, and frozen at –80 °C. The frozen cells were thawed on ice in 100  $\mu$ l lysis buffer (30 mM potassium phosphate, pH 7.7, 50 mM NaCl, 5 mM dithiothreitol (DTT) containing protease inhibitors, 1 mM Pefabloc, 10  $\mu$ g/ml each of aprotinin, leupeptin and Pepstatin A). The cells were disrupted on ice by sonication with a microtip probe (10 pulses), and the homogenate was centrifuged at  $14,000 \times g$  for 10 min followed by at  $100,000 \times g$  for 1 h at 4 °C. The supernatant (cytosol fraction) typically contained 1.1–1.5  $\mu$ g protein/ $\mu$ l. For control assays, cytosol fractions were also prepared from uninfected *Sf9* cells and those expressing *T. cruzi* PFT by co-infection with the viruses carrying *T. cruzi* PFT  $\alpha$  and  $\beta$  genes [16]. For measuring selective formation of a GGPP-protein complex, the cytosol (35  $\mu$ g protein) and 1  $\mu$ l each of ethanol/25 mM  $\text{NH}_4\text{HCO}_3$  (7:3, v/v) containing 0.5  $\mu$ Ci (21.7 pmol) [ $^3\text{H}$ ]GGPP and 50 pmol of unlabeled FPP were mixed in a total volume of 40  $\mu$ l in buffer A (30 mM potassium phosphate, pH 7.7, 100 mM NaCl, and 5 mM DTT). For measuring the formation of a FPP-protein complex, a mixture of 0.5  $\mu$ Ci (19.1 pmol) [ $^3\text{H}$ ]FPP and 50 pmol of unlabeled GGPP was used. The mixture was incubated at 30 °C for 10 min and subjected to gel filtration chromatography at 4 °C on a Superdex 200 HR10/30 column (Pharmacia). Elution was carried out at a flow rate of 0.5 ml/min using buffer A. Fractions of 0.5 ml were collected, and a portion (0.1 ml) was submitted to scintillation counting.

### 2.4. Expression and partial purification of recombinant *T. cruzi* PGGT-I

A suspension culture of *Sf9* cells ( $\sim 1 \times 10^6$  cells/ml) in a spinner flask was infected with baculoviruses of *T. cruzi* PFT  $\alpha$  subunit and *T. cruzi* PGGT-I  $\beta$  subunit at a multiplicity of infection of 1–2. After incubation at 27 °C for 3 days, cells were harvested. The *Sf9* cells from a 10 ml culture were lysed in 1 ml lysis buffer as described above. The lysate was centrifuged at  $14,000 \times g$  for 10 min followed by at  $100,000 \times g$  for 1 h at 4 °C. The resulting supernatant (cytosol fraction, 1.65 mg of protein) was subjected to ammonium sulfate precipitation at 0 °C. The 0–60% ammonium sulfate fraction was dialyzed at 4 °C against 11 of buffer B (20 mM Tris-HCl, 50 mM NaCl, 5 mM DTT, pH 8.0) overnight with three exchanges. The dialyzed material (1.22 mg protein in 447  $\mu$ l) was mixed with 1  $\mu$ Ci of [ $^3\text{H}$ ]GGPP. After incubation at 30 °C for 10 min, the mixture was applied to a column (0.5  $\times$  3.2 cm) of Q-Sepharose HP (Pharmacia) at 4 °C. The column was washed with 3.5 ml of Buffer B at a flow rate of 0.25 ml/min, then a linear gradient elution program was carried out at the same flow rate using buffer B and buffer C (buffer B containing 1 M NaCl); 0–50 min, 0–60% buffer C,

50–52 min, 60–100% buffer C, then 52–72 min, 100% buffer C. Fractions of 0.25 ml were collected, and an aliquot (25  $\mu$ l) of each fraction was counted for radioactivity. For a control experiment, 0.25  $\mu$ Ci of [ $^3\text{H}$ ]GGPP without protein sample in 450  $\mu$ l of buffer A was chromatographed on the same Q-Sepharose HP column as above. Radioactive fractions of the protein · [ $^3\text{H}$ ]GGPP complex (fractions 27–36) were combined and concentrated to 50  $\mu$ l using a Microcon 30 (MILLIPORE).

The concentrated sample (156.8  $\mu$ g protein) was applied to a Superdex 200 HR10/30 column, and chromatography was carried out at 4 °C in 20 mM Tris-HCl, 100 mM NaCl, 5 mM DTT, pH 8.0, containing 0.05%  $\beta$ -octylglucoside at a flow rate of 0.5 ml/min. Fractions of 0.5 ml were collected, and an aliquot (50  $\mu$ l) of each fraction was counted for radioactivity. Fractions 28–30 contained majority of the radioactivity and were pooled and concentrated in a Microcon 30. The concentrated sample contained  $\sim 50$   $\mu$ g protein and stored in buffer containing 10% glycerol at –80 °C. Aliquots of radioactive protein fractions from Q-Sepharose HP and Superdex 200 columns were subjected to protein analysis on SDS-PAGE using a 12.5% gel.

*T. cruzi* PGGT-I apo-enzyme (without bound [ $^3\text{H}$ ]GGPP) was also prepared by the same purification procedures as above. The amount of *T. cruzi* PGGT-I was monitored by SDS-PAGE analysis and by measuring the enzyme activity using the protein substrate H-Ras-CVLL and [ $^3\text{H}$ ]GGPP as describe below. The typical yield of the partially purified *T. cruzi* PGGT-I from 28 ml of *Sf9* cell culture is  $\sim 15$   $\mu$ U ( $\sim 200$   $\mu$ g protein) after the above purification steps. One  $\mu$ unit of PGGT-I activity is defined as 1 pmol product formation per min using H-Ras-CVLL as a substrate. The partially purified enzyme was stored in buffer containing 10% glycerol at –80 °C. The purity was estimated to be  $\sim 90\%$  based on SDS-PAGE analysis.

### 2.5. PGGT-I and PFT assays

Standard reaction mixtures for measuring the geranylgeranyltransferase activity contain 50 ng protein of the partially purified *T. cruzi* PGGT-I or 10 ng protein of rat PGGT-I, 0.65  $\mu$ M (0.3  $\mu$ Ci) [ $^3\text{H}$ ]GGPP and 5  $\mu$ M H-Ras-CVLL in a total volume of 20  $\mu$ l containing 30 mM potassium phosphate, 5 mM DTT, 0.5 mM  $\text{MgCl}_2$ , and 20  $\mu$ M  $\text{ZnCl}_2$ , pH 7.7. After incubation at 30 °C for 30 min, the reaction was terminated by adding 200  $\mu$ l of 10% HCl in ethanol. The amount of radiolabeled protein product was quantified by the glass fiber filter method [8]. When a biotinylated peptide was used as a substrate, the reaction was terminated by boiling for 3 min, and 40  $\mu$ l of avidin-agarose suspension (50% aqueous slurry, Pierce) was added to measure radioactivity transferred to the peptide as described [8]. For PFT assay, 10 ng protein of the recombinant *T. cruzi* PFT was incubated with 0.65  $\mu$ M (0.34  $\mu$ Ci) [ $^3\text{H}$ ]FPP and 5  $\mu$ M of RAS-CVIM or a biotinylated peptide as substrates.

### 2.6. Preparation of cytosol fractions from *T. cruzi* epimastigotes and trypomastigotes

*T. cruzi* epimastigotes (Tulahuen strain) were grown as previously described [30]. Trypomastigotes were obtained by

co-culturing *T. cruzi* with murine 3T3 fibroblasts at 37 °C as previously described [30]. Motile trypomastigotes were recovered from the culture supernatant with virtually no contamination of the adherent mammalian host cells. To prepare cytosol fractions from epimastigotes and trypomastigotes, the cells ( $\sim 1.5 \times 10^8$  cells) were disrupted on ice in 100  $\mu$ l buffer of 30 mM potassium phosphate, pH 7.7, 50 mM NaCl, 10 mM DTT containing protease inhibitors (1 mM Pefabloc, 10  $\mu$ g/ml each of aprotinin, leupeptin, and pepstatin A) by sonication using a microtip probe (10 pulses). The homogenate was centrifuged at  $14,000 \times g$  for 10 min followed by  $100,000 \times g$  for 1 h at 4 °C. The resulting supernatant (cytosol fraction) typically contained 3.5–4.0  $\mu$ g protein/ $\mu$ l.

### 2.7. Northern blot analysis of expression of PGGT-I $\beta$ in different life cycles of *T. cruzi* cells

Northern blots were performed using total RNA from the Tulauen strain trypomastigotes, epimastigotes and the intracellular amastigotes. RNA was purified using the RNeasy Mini kit and Qiashredder column (Qiagen, Valencia, CA). Amounts of RNA loaded were 13  $\mu$ g for the epimastigotes and trypomastigotes, and 70  $\mu$ g for amastigotes/mouse 3T3 fibroblast host cells (in which 15–20% was estimated to be from the amastigotes). Total RNA from uninfected fibroblasts (30  $\mu$ g) was loaded as a negative control. Blots were hybridized with a PCR generated DNA probe corresponding to bases 718–967 of the *T. cruzi* PGGT-I  $\beta$  gene or bases 651–1319 of the *T. cruzi* 18S ribosomal RNA (GenBank AF288660). The relative expression levels were quantified by densitometry and normalized against the 18S ribosomal RNA band densities.

## 3. Results and discussion

### 3.1. Cloning and sequence analysis

BLAST similarity searching of the *T. cruzi* gene database [28] with mammalian and yeast PGGT-I  $\beta$  protein sequences led to identification of an open reading frame (ORF) of Tc00.1047053508817.150 (1383 bp) annotated as a “conserved hypothetical” protein. The deduced amino acid sequence showed low identity (19–23%) to rat PGGT-I  $\beta$  and PGGT-II  $\beta$  sequences, but it contained several residues that are unique in PGGT-I  $\beta$  as described below. Analysis of the cDNA to establish the correct boundaries of the gene expressed *in vivo* revealed that the actual start ATG occurs at nucleotide position 178–180 of Tc00.1047053508817.150. There is a typical splice leader acceptor site (i.e. polypyrimidine track followed by an AG dinucleotide at position 135–136) [31] downstream of the GeneDB predicted start ATG. Of particular interest for the actual cDNA, there are two start codons 37 and 42 nucleotides downstream of the spliced-leader sequence. These two ATGs are in different reading frames, and the first ATG is in a short ORF of 27 bp, whereas the second ATG gives the full ORF of 1206 bp whose translated amino acid sequence is shown in Fig. 1. The significance of the first

short ORF is unknown. A very low level of PGGT-I activity was detectable in the cytosol fraction of *T. cruzi* epimastigotes [26]. It is possible that this gene architecture may allow for low expression levels of the PGGT-I  $\beta$  since the ribosome could preferentially begin translation at the first start codon.

Fig. 1 shows comparison of the amino acid sequences between three  $\beta$  subunits of protein prenyltransferases, PFT, PGGT-I, and PGGT-II from *T. cruzi* and rat, including the putative *T. cruzi* PGGT-I  $\beta$  subunit. All three of the zinc binding residues, Asp269, Cys271, and His321 (residue numbers in rat PGGT-I  $\beta$ ) are conserved in all of these prenyltransferase  $\beta$  subunits (Fig. 1). The putative *T. cruzi* PGGT-I  $\beta$  sequence contains several unique residues including Phe53 and Lys311 that are conserved in PGGT-I  $\beta$  orthologs from rat and 12 other species but not in PGGT-II  $\beta$  or PFT  $\beta$  orthologs from rat (Fig. 1) and most of other species (not shown). Structural studies with mammalian PGGT-I and PFT revealed the residues contacting GGPP or FPP [9] that include the consensus residues Phe53 and Lys311 in PGGT-I  $\beta$  (Fig. 1). Trp102 and Tyr365 in the mammalian PFT  $\beta$  subunit have been shown to block binding of GGPP by steric hindrance of the bulky side groups based on the crystal structure and mutational studies [9,32]. The residues corresponding to Trp102 and Tyr365 are altered in the putative *T. cruzi* PGGT-I  $\beta$  as in the rat PGGT-I ortholog (Fig. 1). Among residues of the rat enzymes contacting CaaX peptide substrates, His121 and Ala123 of rat PGGT-I  $\beta$  are altered to Thr and Ser in the *T. cruzi* sequence (Fig. 1). Thus, the putative *T. cruzi* protein shows significant identity to PGGT-I  $\beta$  orthologs, although substantial differences in residues contacting substrates from those of rat enzyme are present, suggesting unique substrate specificity of *T. cruzi* PGGT-I.

### 3.2. Expression of the putative *T. cruzi* PGGT-I in *Sf9* insect cells

PGGT-I enzymes that have been characterized consist of a  $\beta$  subunit tightly bound to an  $\alpha$  subunit, which is identical to the  $\alpha$  subunit of PFT. Co-expression of the putative *T. cruzi* PGGT-I  $\beta$  and *T. cruzi* PFT  $\alpha$  subunit genes was carried out in the baculovirus/*Sf9* cell system. Detection of the protein expression was done by immuno-blotting analysis using antiserum that was raised against a synthetic peptide corresponding to the predicted amino acid residues 63–79 of the putative PGGT-I  $\beta$  gene. A high level of protein with apparent molecular weight of 42 kDa, similar to the calculated molecular weight of the putative *T. cruzi* PGGT-I  $\beta$  (44.5 kDa), was detected in the cytosol fraction obtained from the infected *Sf9* cells (Fig. 2A, lane 1). No significant western blot band was seen in a control sample from *Sf9* cells co-infected with baculoviruses of *T. cruzi* PFT  $\alpha$  and  $\beta$  subunits (Fig. 2A, lane 2), although bands of the PFT  $\alpha$  and  $\beta$  subunits (apparent molecular weights of  $\sim 68$  and 70 kDa) were seen in the gel stained with Coomassie blue (not shown). This shows that a significant expression level of the putative *T. cruzi* PGGT-I  $\beta$  protein was obtained in *Sf9* cells when co-expressed with the PFT  $\alpha$  subunit.

Rat PGGT-II	-----MGTOQKDVITK	11
T. cruzi PGGT-II	-----MA	2
Rat PFT	MASSSSFTYYCPSSSPVWSEPLYSLRPEHARERLQDDSVETVTSIEQAKVEEKIQEVFS	60
T. cruzi PFT	MAAYVGSVPFATLTTLAQREVELSLLQFLRQYHPKVDELWRTHPDAEPMETVEEMCMDAS	60
Rat PGGT-I	-----MAATEDDRLA	10
T. cruzi PGGT-I	-----MPHAVVVMG	9
Rat PGGT-II	SDAPDTLL--EKHADYIASYGSKDD--YEYCMSEYLRMSGVYWGTLVMDLMGQLHRM	66
T. cruzi PGGT-II	EEVSKRLLA--DLHLKFLGLDEKKDD--LRYWMSQHLKVS GAFWGLSAMELLGLHLDKI	57
Rat PFT	SYKFNHLVPRLLVQREKHFHYLKRGRQLTDAYECLDASRPFVLCYWIHLSLELLDEPIFQ	120
T. cruzi PFT	DDCKGDHLP--RLHRELHDSYVQGRFLGEGSTOGLYSSQFVWLAFWALQADVDLITEEL	118
Rat PGGT-I	GSGERLD---FLRDRHVRFFQRCLQVLPERYSSLETSRLTIAFFALSGLDMLDSDLV	67
T. cruzi PGGT-I	EDETSQILG---DGFVHLQYFSPNQRCPAKVQQQHSQRI I LLYF SLLGRDLLGVDRK	66
		* * #
Rat PGGT-II	NKEE-----ILVFIKSCQHEC-----	82
T. cruzi PGGT-II	NRQD-----VIEFVVGWNSD-----	73
Rat PFT	IVAT-----DVCQFLELCQSPD-----	137
T. cruzi PFT	YEHVS---PDALGNF ILGCLQEVKKS GTSNDDDMRNNPMDMEQESVLLRNPFVSI FDDD	175
Rat PGGT-I	NKDDI---IEWIYSLQVLPTEDRSNLDRCGFRGSSYLGI PFNPSK-----	109
T. cruzi PGGT-I	DDGVFNAERDKLFEEMRRCYDTETGG-----	92
Rat PGGT-II	-----GGVSASIGHDPHLLYTL SAVQILTYD-----SIHVINVDKVVA YVQSLQKE	129
T. cruzi PGGT-II	-----GGFGGNGQDSHMLYTL SAVOVLCLLG-----ALNAIDKEKACACWASMQLP	120
Rat PFT	-----GGFGGGGQYPHLAPTAAVNALCIIGTE--EAYNVINREKLLQYL YSLRQP	187
T. cruzi PFT	NDDGKRLVGFAGGQLA QIPHLAAS YAALCSLCILPRT--TYLRALPRAAIKRWLLSLRCK	233
Rat PGGT-I	-----NPGTAHPYDSGHIA M Y TGLSCL I ILG---DDL SRV DKEACLAGLRALQLE	157
T. cruzi PGGT-I	-----FCPVVSHYNTSATLSMTHCALQILNLCDFLPKATEWYKEKLM SFVMSCHIR	146
		o o *
Rat PGGT-II	-----DGSFAGDIWG-EIDTRF SFC AVATLALL-----GKLDAINVEKAI	168
T. cruzi PGGT-II	-----DGSFQGDENG-EVDTRFVYIAMNCLQLL-----GRLHLIDLDAV	159
Rat PFT	-----DGSFLMHVGG-EVDVRSAYCAASVASLT-----NIITPDLFEGTA	226
T. cruzi PFT	-----DGSFCHMTGG-EADIRASYCVAVMTVLLQLNDVPA YTDGRDDTVITEQTA	282
Rat PGGT-I	-----DGSFC AVPEGSENDMR FVY CASCI CYMLN-----NWSGMDMKKA	197
T. cruzi PGGT-I	HECPLFGESFRGAFQAAPDIAEVDIRFTYSALVSMALLCKPQ--PLSTVSSLQGTLEAV	204
		# **
Rat PGGT-II	EFVLSMNFDDGGFCRP-GSESHAGQIYCTGFLAITSQLHQVNSD-LLGWLRCERQLP-	225
T. cruzi PGGT-II	RWVLCQONWDGGFGVAP-GAESHAGQIFCCVVGALS IANALHCIDKE-QLSSWLAMRQLP-	216
Rat PFT	EWIARCONWEGGIGVVP-GMEAHGGYTFGLAALVILKKERSLNLK-SLLQWVTSRQMRP	284
T. cruzi PFT	AFVASCQTHEGGFACGLNASEAHGAYTQCGLAALILMRS PHLCKYA-ALRRVLSARQLKF	341
Rat PGGT-I	SYIRMSYDNGLAQGA-GLESHGGSTFCGIASLCLMGKLEEVFSEKELNRKRWCIMRQ	256
T. cruzi PGGT-I	AFIWRWDAHEGAFGAVPGAEAHGGMTFC AVASLALAGAMSSLTRS-RHLLLLRYCTARL	263
		o * * * *
Rat PGGT-II	SGGLN-----GRPEKLPVVCYSWVWLASLKII-----	252
T. cruzi PGGT-II	SGGLN-----GRPEKAVVCYSWVWVSSLSML-----	243
Rat PFT	EGGFQ-----GRCNKLVDGCYSFWQAGLLP L LHR-----	313
T. cruzi PFT	EGGFN-----GRTNKLVDSCYSYVWVWASHMLLRVGESYMRLLGQPTET	383
Rat PGGT-I	QNGYH-----GRPNKPVDTYCFVFWGATLKLK-----	284
T. cruzi PGGT-I	SGGPEDHESIGSTGVIMPVIGYQGRPQKEDTQYSHWIGSTLRILQT-----	310
		* * # # * *
Rat PGGT-II	-----GRLHWIDREKLRSLF ILACQDEETGGFADRPDGMVDVFFITLFGIAGLSLL	301
T. cruzi PGGT-II	-----GHTDWIDRKALFNF ILACQDAEDGGISDKPGNMADVFFYGLCGLSLL	292
Rat PFT	ALHAQGDPA LMSHMFHQALQEY ILMCCQCPAGLLDKPGKSRDFYETCYCLSGLSIA	373
T. cruzi PFT	TVTQSFLDEDVDFYFNQRLLLYLVLSCCQDKEMGGLMDKPGCLNDAYETCYSLSGMSTA	503
Rat PGGT-I	-----IFQYTNFEKRNRY ILSQDRLVGGFAKWPDSHPDALHAYFGICGLSML	332
T. cruzi PGGT-I	-----QEHDVFPVDVLP IFRFMGNCVDSEHGGIRKDFDMRADIVHSLGLSGLLLH	362
		o o # *
Rat PGGT-II	GEEQ---IKPVSPVFCMPEEVLQRVNVQPELVS-----	331
T. cruzi PGGT-II	GYEDYP--LNEINPVYAMPYSVLEELGVPEERGLHV GKARREKA-----	334
Rat PFT	QHFG-S--GAMLHDVVMGPENVLQPTHPVYINIGPDKVIQATHTFLQKVPVGFEECEDAVT	430
T. cruzi PFT	QNLQYL--PRSCNTDLMYATALRRGYIPNERDDYEIVLAAHNSNSGVGGGCCRQERLS	561
Rat PGGT-I	EESG---ICKVHPALNVSTRT SERLRLDLHQSWKTKDSKQCSDNVHISS-----	377
T. cruzi PGGT-I	VDSHCVSKLRPPHPVYGCWSVTRNTGLPELVATSTTL-----	401
		*

Fig. 1. Comparison of amino acid sequences between the three protein prenyltransferase  $\beta$  subunits from *T. cruzi* and rat. Alignment was made using Clustal W program with the putative *T. cruzi* PGGT-I  $\beta$  (GenBank accession number EU113181) and PGGT-II  $\beta$  (XP\_817693), *T. cruzi* PFT  $\beta$  (AAL69905) (residues 383–442 and 562–588 that do not align with others are not shown), rat PGGT-I  $\beta$  (AAA17756), PGGT-II  $\beta$  (AAA41999), and PFT  $\beta$  (AAA41176) (residues 431–436 are not shown). The conserved three residues binding to the active site Zn<sup>2+</sup> ion are indicated as letters in black boxes. Trp102 and Tyr365 (numbers from rat PFT  $\beta$ ) shown in open boxes are reported to be involved in specific FPP binding [32]. Phe53 and Lys311 (numbers from rat PGGT-I  $\beta$ ) shown in open boxes are consensus residues among PGGT-I  $\beta$  orthologs from most species. Residues of mammalian PGGT-I  $\beta$  or PFT  $\beta$  contacting GGPP or FPP (\*), those contacting the CaaX peptide (°), or both (#) are indicated below the alignment (according to ref. [9]).

### 3.3. Analyses for expression of the putative PGGT-I $\beta$ gene in different life-cycle stages of *T. cruzi* cells

Northern blots demonstrate that the putative PGGT-I  $\beta$  gene is transcribed in three separate life-cycle stages of *T. cruzi* (Fig. 3). The level of the PGGT-I  $\beta$  mRNA slightly varies between mammalian stage infectious trypanomastigotes, intracellular amastigotes grown in mouse 3T3 cells, and insect stage epimastigotes.

When cytosol fractions from the three life-cycle stages of *T. cruzi* cells were subjected to immuno-blotting analysis using the same antiserum as in Section 3.2, a band co-migrating with the recombinant PGGT-I  $\beta$  protein was detected in all three life-cycle cells tested but not in the mouse host cells (Fig. 2B). The results suggest that the putative PGGT-I  $\beta$  gene is expressed at the protein level in *T. cruzi* cells with somewhat varied levels between the different life-cycle stages.

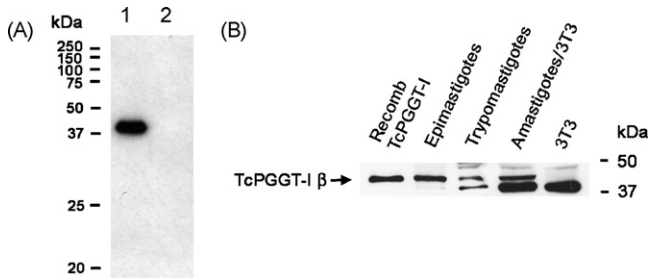


Fig. 2. Western blot analysis. (A) Expression of the recombinant putative *T. cruzi* PGGT-I  $\beta$  in *Sf9* cells. Cytosolic proteins from *Sf9* cells co-expressing the putative *T. cruzi* PGGT-I  $\beta$  and PFT  $\alpha$  subunit genes (lane 1) or *T. cruzi* PFT  $\alpha$  and  $\beta$  subunit genes (lane 2) were resolved by SDS-PAGE using an 11% gel. (B) Detection of the putative PGGT-I  $\beta$  protein in *T. cruzi* cells. Cytosolic proteins from *T. cruzi* epimastigotes, trypomastigotes, amastigotes/mouse 3T3 cells, and uninfected mouse 3T3 cells (amounts loaded are 8, 8, 28, and 24  $\mu$ g protein, respectively) were subjected to the analysis. Partially purified recombinant *T. cruzi* PGGT-I (10 ng) was loaded as a standard, and the arrow indicates the migration position of the  $\beta$  subunit. Immunoblotting was performed with rabbit antiserum raised against the synthetic peptide corresponding to residues 63–79 (VDWRKDDGVFNAERDKL) of the putative *T. cruzi* PGGT-I  $\beta$ . Horseradish peroxidase-conjugated anti-rabbit IgG antibody was used as a secondary antibody, and the enhanced chemiluminescent reagent (Amersham) was used to visualize the protein band.

### 3.4. Formation of the enzyme-GGPP complex

Mammalian PGGT-I and PFT have been shown to form a tight complex selectively with GGPP and FPP, respectively, that can be isolated by gel filtration chromatography [7,8]. To explore the possible formation of a protein-GGPP complex, cytosolic proteins from *Sf9* cells expressing the recombinant proteins were incubated briefly with [ $^3$ H]GGPP and unlabeled FPP (~2 mol excess), and the complex formation was analyzed by Superdex 200 gel filtration chromatography. Unlabeled FPP was added to measure specific [ $^3$ H]GGPP-binding, since mammalian PGGT-I is known to selectively bind GGPP over FPP with affinity for GGPP ~300-fold higher than for FPP [8]. Mammalian PFT has also been shown to form a tight complex with FPP with binding affinity ~15-fold higher than GGPP [8]. For measuring selective complex formation with FPP, a mixture of [ $^3$ H]FPP and unlabeled

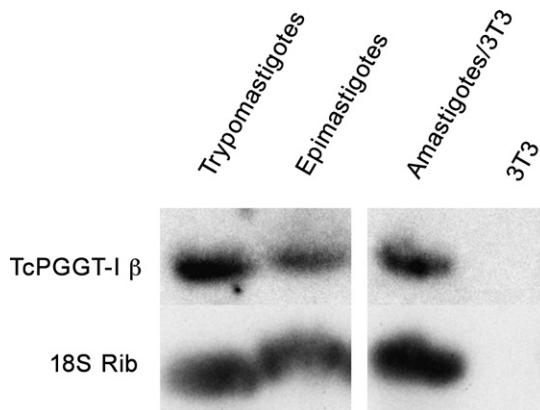


Fig. 3. Northern blot analysis. Total RNAs from *T. cruzi* trypomastigotes, amastigotes/mouse 3T3 fibroblasts, epimastigotes, or control mouse 3T3 fibroblast cells were blotted and hybridized with a probe for the *T. cruzi* PGGT-I  $\beta$  subunit (top) or the *T. cruzi* 18S ribosomal RNA (bottom).

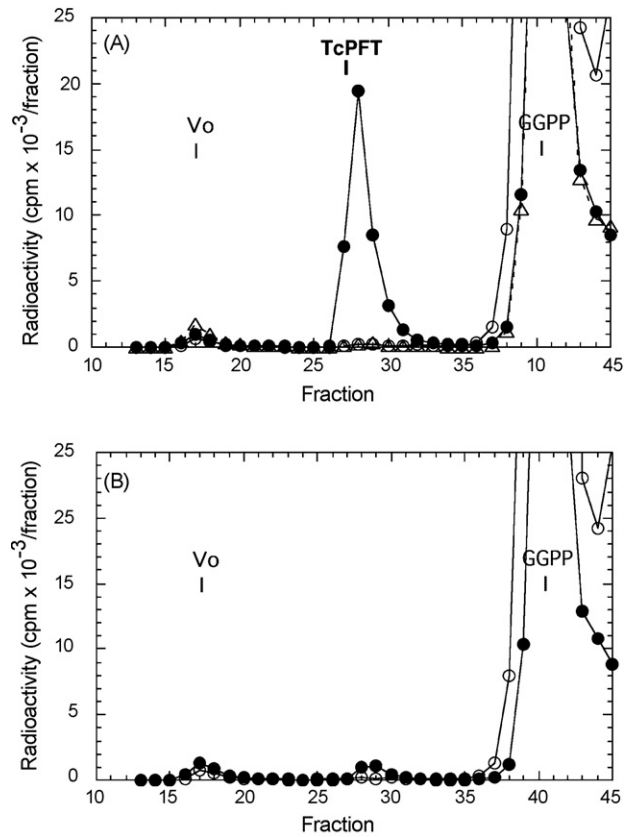


Fig. 4. Formation of a GGPP-enzyme complex. (A) The cytosol (35  $\mu$ g protein) from *Sf9* cells co-infected with the baculoviruses carrying the putative *T. cruzi* PGGT-I  $\beta$  and PFT  $\alpha$  subunit genes was used to examine the complex formation with [ $^3$ H]GGPP ( $\bullet$ ) or with [ $^3$ H]FPP ( $\circ$ ). The cytosol from *Sf9* cells infected with a virus carrying the putative *T. cruzi* PGGT-I  $\beta$  alone was also tested for [ $^3$ H]GGPP complex formation ( $\Delta$ ). For detecting selective complex formation with either GGPP or FPP, the cytosol samples were incubated at 30  $^{\circ}$ C for 10 min with a mixture of either 0.5  $\mu$ Ci (21.7 pmol) [ $^3$ H]GGPP and 50 pmol of unlabeled FPP or 0.5  $\mu$ Ci (19.1 pmol) [ $^3$ H]FPP and 50 pmol of unlabeled GGPP, respectively. The mixture (40  $\mu$ l) was subjected to gel filtration chromatography on a Superdex 200 HR10/30 column. (B) The cytosol from uninfected *Sf9* cells was used for the complex formation with [ $^3$ H]GGPP ( $\bullet$ ) or with [ $^3$ H]FPP ( $\circ$ ). The void volume (Vo), and elution positions of *T. cruzi* PFT and GGPP are indicated. FPP eluted at fraction 46.

labeled GGPP (~2 mol excess) was used. As shown in Fig. 4A, the cytosol fraction from *Sf9* cells co-expressing the putative *T. cruzi* PGGT-I  $\beta$  and the PFT  $\alpha$  subunits gave a radioactive protein peak with [ $^3$ H]GGPP that eluted at a position corresponding to a molecular weight slightly smaller than that of *T. cruzi* PFT protein. The cytosolic proteins from uninfected *Sf9* cells (Fig. 4B) or those infected only with a baculovirus carrying the putative *T. cruzi* PGGT-I  $\beta$  gene (Fig. 4A) produced only low amounts of the radioactive protein peak, which may represent the endogenous level of *Sf9* PGGT-I. Formation of a protein-[ $^3$ H]FPP complex was not detectable with the same cytosolic protein sample of *Sf9* cells expressing the putative *T. cruzi* PGGT-I  $\beta$  and the PFT  $\alpha$  subunits (Fig. 4A). Thus, the results suggest that selective formation of a protein-[ $^3$ H]GGPP complex occurs with a dimeric protein of the putative *T. cruzi* PGGT-I  $\beta$  and the PFT  $\alpha$  subunits.

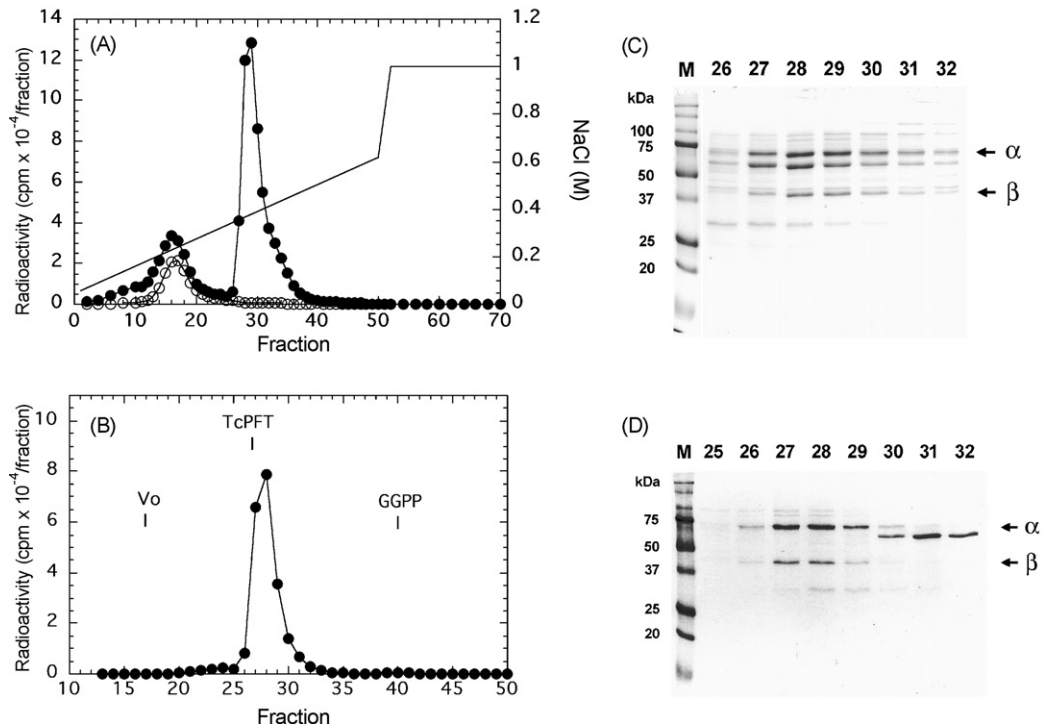


Fig. 5. Isolation of [ $^3\text{H}$ ]GGPP · enzyme complex. (A) Q-Sepharose chromatography. The dialyzed 60% ammonium sulfate fraction (1.22 mg protein) of cytosol from *S9* cells expressing the putative *T. cruzi* PGGT-I  $\beta$  and PFT  $\alpha$  was mixed with  $1 \mu\text{Ci}$  of [ $^3\text{H}$ ]GGPP and chromatographed on a Q-Sepharose HP column ( $0.5 \times 3.2 \text{ cm}$ ) ( $\bullet$ ). Aliquots of fractions were counted for radioactivity. Elution profile of [ $^3\text{H}$ ]GGPP (0.25  $\mu\text{Ci}$ ) alone is also shown ( $\circ$ ). (B) Superdex 200 gel filtration chromatography. The radioactive protein (fractions 27–30) from the Q-Sepharose chromatography (Fig. 4A) was concentrated and applied to a Superdex 200 HR10/30 column. Elution positions of *T. cruzi* PFT, GGPP, and void volume are indicated. (C) Protein analysis of the radioactive protein peak from Q-Sepharose column (A). Aliquots of fractions 26–32 were subjected to SDS-PAGE analysis using a 12.5% gel, and protein bands were visualized by Coomassie blue staining. (D) Protein analysis of the radioactive peak from Superdex 200 column (B). Fractions 25–32 were subjected to SDS-PAGE analysis. Arrows indicate the putative migration positions of the  $\alpha$  and  $\beta$  subunit proteins. Protein molecular weight markers are shown in the left lanes (M).

### 3.5. Co-purification of the putative *T. cruzi* PGGT-I $\beta$ with PFT $\alpha$ and [ $^3\text{H}$ ]GGPP as a ternary complex

We further investigated whether the putative *T. cruzi* PGGT-I  $\beta$  and the PFT  $\alpha$  subunit form a dimeric protein that binds GGPP. To isolate the protein·[ $^3\text{H}$ ]GGPP complex, 60% ammonium sulfate precipitated proteins from the cytosol of *S9* cells expressing the two subunits were mixed with [ $^3\text{H}$ ]GGPP, and the mixture was subjected to two steps of chromatography. As shown in Fig. 5A, two radioactive peaks were separated after Q-Sepharose ion exchange chromatography. The elution position of a peak at  $\sim 0.3 \text{ M}$  NaCl corresponds to that of [ $^3\text{H}$ ]GGPP alone in the same column. Fractions of a large radioactive peak eluted at  $\sim 0.4 \text{ M}$  NaCl were subjected to protein analysis on SDS-PAGE. This showed co-elution of a few proteins with [ $^3\text{H}$ ]GGPP (Fig. 5C). Further purification of the radioactive protein peak by Superdex 200 gel filtration chromatography followed by SDS-PAGE analysis revealed two protein bands with apparent molecular weights of  $\sim 42.5$  and  $70 \text{ kDa}$  that co-eluted with [ $^3\text{H}$ ]GGPP (Fig. 5B and D). The calculated molecular weights of the putative *T. cruzi* PGGT-I  $\beta$  and the PFT  $\alpha$  subunits are  $\sim 44.5$  and  $72.5 \text{ kDa}$ , respectively, which agree with band positions in the SDS-PAGE. These results indicate that a dimeric protein consisting of the putative *T. cruzi* PGGT-I  $\beta$  and the PFT  $\alpha$  subunits forms a complex with [ $^3\text{H}$ ]GGPP.

### 3.6. Protein geranylgeranyltransferase activity of the recombinant enzyme

The radioactive peak containing the putative *T. cruzi* PGGT-I  $\beta$  and the PFT  $\alpha$  subunits obtained from Superdex 200 chromatography (Fig. 5B) was tested for the enzyme activity of transferring a geranylgeranyl group from GGPP using a panel of mammalian and yeast protein substrates (Table 1). The partially purified protein showed significant amounts of [ $^3\text{H}$ ]geranylgeranyl-transferring activity on most of the C-terminal CaaX-containing proteins ending with Leu or Met. However, a very small amount of activity was detected with those substrates having X = Phe or RhoB-CKVL. This result illustrates the different CaaX specificity from that of mammalian PGGT-I (Table 1). The proteins with X = Met were also good substrates for *T. cruzi* PFT, and one with X = Cys was selectively utilized by PFT. Two mammalian Rab family GTPases lacking the CaaX motif but containing the C-terminal CXC sequence did not serve as substrates for *T. cruzi* PGGT-I as expected.

### 3.7. Substrates for the putative *T. cruzi* PGGT-I in *T. cruzi* cells

To identify *T. cruzi* proteins with C-terminal CaaX sequences as potential substrates of *T. cruzi* PGGT-I or PFT, BLAST

Table 1  
Activity of *T. cruzi* PGGT-I and PFT on several protein substrates of mammalian and yeast protein prenyltransferases

Protein substrate	Prenyl-group transferred (fmol/30 min)		
	<i>T. cruzi</i> PGGT-I	Rat PGGT-I	<i>T. cruzi</i> PFT
H-Ras-CVLS	0	0	9.7
H-Ras-CVLL	204.0	151.6	3.3
RAS1-CAIL	278.8	n.d.	0.3
Rap2B-CVLL	194.9	204.7	n.d.
RhoB-CKVL	3.3	154.3	n.d.
RAS1-CVIM	141.2	113.6	142.8
K-Ras-CVIM	166.3	99.0	161.0
GST-CDC42-CCIF	5.5	26.6	0
GST-TC21-CVIF	0	111.1	0
RAS2-CIIC	0	n.d.	50.5
Rab3A-CAC	0	0	0
Rab6-CSC	0	0	0

Each protein (5  $\mu$ M) was incubated at 30 °C for 30 min with either partially purified *T. cruzi* PGGT-I (50 ng protein) and 0.65  $\mu$ M (0.3  $\mu$ Ci) [<sup>3</sup>H]GGPP or *T. cruzi* PFT (10 ng protein) and 0.65  $\mu$ M (0.34  $\mu$ Ci) [<sup>3</sup>H]FPP. Rat PGGT-I (10 ng protein) was also assayed with these proteins under the same conditions for comparison. Control levels without protein substrate or enzyme were 7.7 and 2.8 fmol for PGGT-I and PFT assays, respectively, which were subtracted from the data. The typical experimental error is <10%. n.d.: not determined.

searching was carried out against the *T. cruzi* genome in GeneDB using several mammalian prenylated proteins such as human Ras superfamily small GTPases as queries. As shown in Table 2, the search revealed at least five small GTPase-like proteins that have C-terminal CaaX tetrapeptide sequences, which include previously reported TcRho1 GTPase with C-terminal CQLF [26]. By sequence alignment of these putative *T. cruzi* GTPase-like proteins with human GTPases (not shown), XP\_818107 was

Table 2  
Candidate protein substrates of *T. cruzi* PGGT-I and PFT

Protein name/accession number	CaaX sequence	Reference and comment
Small GTPase-like protein		
XP_818107	CVLL	Ras-like protein
XP_814824	CTLL	
XP_819513	CHFM	
TcRho1 (AAG09284)	CQLF	Farnesylated [26]
XP_818500	CWLM	Putative Rab28 homolog [37]
PRL protein tyrosine phosphatase		
TcPRL-1 (AAS19277)	CAVM	Farnesylated [27]
XP_815396	CTLM	
XP_805262	CTVM	
XP_816678	CIVM	
DNAJ		
Tcj2 (AAC18895)	CTQQ	[36]
Tcj4 (AAC18897)	CQLQ	[36]
XP_819443	CAHQ	
XP_818454	CVHQ	
XP_820422	CAAQ	

Shown are putative or characterized *T. cruzi* proteins containing the C-terminal CaaX sequence found in the gene database; homologs of small GTPase-like proteins, PRL (phosphatase found in regenerating liver) protein tyrosine phosphatases, and DNAJ proteins.

found to be highly similar to human H-, K-, N-Ras and Rap proteins (42–47% sequence identity). In addition, this protein contains sequences similar to the conserved switch 1 and switch 2 domains, YDPTIED (residues 32–38) and GQEEYSAMRDQYMRTG (residues 60–75), respectively, of human Ras proteins [33]. In the *T. cruzi* putative protein, the sequences that align with the switch 1 and switch 2 are YDATIED and GQDAFGAMRDQYLKKG, respectively. The residue Gln61 of Ras proteins is involved in GTP hydrolysis and an oncogenic mutation site, while Thr is the natural residue at this position in Rap proteins [34]. This Gln residue is conserved in XP\_818107. These suggest that this *T. cruzi* protein is an ortholog of Ras family GTPases.

BLAST gene database searching with TcPRL-1 and human PRL sequences identified three PRL homologs in *T. cruzi*, which show ~35–41% sequence identity to human PRL-1, 2 and 3, and contain the conserved catalytic region sequence HCVAGLGRAP [35]. All of these four *T. cruzi* PRL homologs contain the C-terminal CaaX sequence ending with Met, and thus are predicted to be prenylated similarly to TcPRL-1, which has been reported to be farnesylated [27]. Two *T. cruzi* DNAJ proteins (Tcj2 and Tcj4) that have previously been reported also contain the CaaX sequences [36]. By BLAST search with the Tcj2 and Tcj4 sequences, three additional putative DNAJ proteins with the CaaX motif were found in *T. cruzi*, which show 24–44% sequence identity to Tcj2 or Tcj4, and contain three to four repeats of the conserved Zinc finger motif CXXCXGXG and the J-domain motif HPD (the latter is not present in XP\_820422). All these proteins contain the CaaX motif ending with Gln, which are expected to be substrates for *T. cruzi* PFT since the SSCALQ peptide was one of the best substrates of *T. cruzi* PFT among 20 different peptides of SSCALX (X is one of 20 different amino acids) as described previously [16].

The C-terminal peptides of the Ras-like protein with CVLL and the GTPase-like protein with CHFM as well as those of CTQQ (Tcj2), CQLF (TcRho1) and CAVM (TcPRL-1) were tested as substrates for either *T. cruzi* PGGT-I or PFT (Table 3). Among these, only a peptide of the Ras-like protein with CVLL was efficiently geranylgeranylated by *T. cruzi* PGGT-I, while others containing C-terminal CTQQ, CAVM, CHFM and CQLF were selectively farnesylated by *T. cruzi* PFT. It is notable that no significant prenylation cross-over by *T. cruzi* PGGT-I and PFT occurs for these C-terminal peptides, unlike a number of mammalian protein substrates with X = Met reported to be prenylated by both of mammalian enzymes *in vitro* and *in vivo* [4]. The peptides with CAVM and CHFM were modified by *T. cruzi* PFT but not by PGGT-I, although K-Ras-CVIM and RAS1-CVIM proteins served as good substrates for both *T. cruzi* PGGT-I and PFT (Table 1). These results suggest that additional factors other than the X-residue dictate the selectivity of recognition by PFT versus PGGT-I.

Further studies on specificity of *T. cruzi* PGGT-I were carried out in comparison with that of PFT. Partially purified apoenzyme of *T. cruzi* PGGT-I and [<sup>3</sup>H]GGPP were shown to form a significant amount of the complex separated by Superdex 200 chromatography (Fig. 6A) as seen in the experiment using the

Table 3  
 Prenylation specificity of C-terminal peptides of putative *T. cruzi* protein substrates

Substrates		Prenyl-group transferred (fmol/15 min)		Protein
Biotin-peptide	Prenyl donor	<i>T. cruzi</i> PGGT-I	<i>T. cruzi</i> PFT	
KKRRCVLL	GGPP	393.4 ± 33.5	36.9 ± 11.4	Ras-like protein
	FPP	105.1 ± 13.4	34.4 ± 14.0	
TGATCTQQ	GGPP	8.3 ± 6.3	15.0 ± 6.6	Tcj2
	FPP	4.4 ± 1.3	601.8 ± 67.7	
SCAGCAVM	GGPP	6.7 ± 4.4	22.2 ± 12.3	TcPRL-1
	FPP	5.4 ± 2.4	984.9 ± 40.0	
QCRRCHEFM	GGPP	4.0 ± 2.6	19.7 ± 5.3	Small GTPase-like protein
	FPP	9.0 ± 1.0	707.5 ± 94.6	
QSCQLF	GGPP	15.3 ± 10.2	n.d.	TcRho1
	FPP	n.d.	215.5 ± 41.1	

Recombinant *T. cruzi* PGGT-I (50 ng protein) or *T. cruzi* PFT (20 ng protein) was incubated at 30 °C for 15 min with 5 μM of the biotinylated peptide and 0.65 μM of either [<sup>3</sup>H]GGPP (0.3 μCi) or [<sup>3</sup>H]FPP (0.34 μCi). The data represent mean ± the standard deviations of two independent measurements. Control levels without peptide substrate are 73.9 ± 14.2 and 63.0 ± 5.6 fmol, respectively, for [<sup>3</sup>H]geranylgeranyl transfer and [<sup>3</sup>H]farnesyl transfer assays, which were subtracted from the data. n.d.: not determined.

cytosol of *Sf9* cells co-expressing the α and β subunits (Fig. 4A). In contrast, despite its high specificity for FPP over GGPP in the transferase reaction, *T. cruzi* PFT was unable to form a significant level of a tight complex with [<sup>3</sup>H]FPP under the conditions that rat PFT can efficiently form the complex with [<sup>3</sup>H]FPP (Fig. 6B and C). A very low level of PFT·[<sup>3</sup>H]FPP complex formation was also observed with the cytosol from *Sf9* cells expressing *T. cruzi* PFT α and β subunits (not shown), suggesting a relatively low affinity of FPP to *T. cruzi* PFT.

*T. cruzi* PGGT-I shows preferential utilization of GGPP but can also utilize FPP to prenylate the CVLL peptide, whereas *T. cruzi* PFT is highly selective for the utilization of FPP (Table 3). Kinetic studies of prenylation of the CVLL peptide by *T. cruzi* PGGT-I showed that the apparent  $K_M$  values for GGPP and FPP are similar (~0.5 μM), but the  $V_{max}$  value with GGPP is three to four fold higher than the  $V_{max}$  with FPP (Fig. 7A). It was also found that the peptide with C-terminal CVLL shows higher affinity to *T. cruzi* PGGT-I over PFT with a ~4-fold lower  $K_M$  value for *T. cruzi* PGGT-I (Fig. 7B and Table 4). Thus, the C-terminal peptide containing CVLL of the *T. cruzi* Ras-like protein is selectively geranylgeranylated *in vitro* by *T. cruzi* PGGT-I. A tight and selective binding to GGPP (Fig. 4A) may contribute largely to the specific action of *T. cruzi* PGGT-I in cells as suggested for mammalian PGGT-I [8].

Table 4

The  $K_M$  values for *T. cruzi* PGGT-I and PFT acting on the C-terminal CaaX peptides of the putative *T. cruzi* protein substrates

Biotin-peptide	$K_M$ (μM)	
	<i>T. cruzi</i> PGGT-I	<i>T. cruzi</i> PFT
KKRRCVLL	1.0 ± 0.1	4.0 ± 0.7
TGATCTQQ	n.d.	3.7 ± 1.7
SCAGCAVM	n.d.	3.9 ± 0.6
QCRRCHEFM	n.d.	4.2 ± 1.5

The standard assays for PGGT-I and PFT were performed with various concentrations of each biotinylated peptide. The  $K_M$  values for the peptides were determined by fitting the data to the Michaelis–Menten equation using non-linear regression. The values represent mean ± S.D. of two independent measurements. n.d.: not determined due to low activity.

### 3.8. PGGT-I activity in *T. cruzi* trypomastigotes (mammalian stage) and epimastigotes (insect stage)

PGGT-I and PFT assays were carried out with the cytosol fractions from *T. cruzi* cells (trypomastigotes and epimastigotes) (Table 5). Using a large amount of cytosolic protein (9 μg) and a prolonged incubation (30–120 min), low but reproducible levels of PGGT-I activity were detectable using H-Ras-CVLL or RAS-CVIM as a substrate. Both trypomastigotes and epi-

Table 5  
 PGGT-I and PFT activities in *T. cruzi* trypomastigotes (mammalian stage) and epimastigotes (insect stage)

<i>T. cruzi</i> cells	Protein substrate	PGGT-I activity (fmol/min μg protein)	PFT activity (fmol/min μg protein)
Trypomastigotes	H-Ras-CVLL	0.018 ± 0.003	0.007 ± 0.002
	RAS-CVIM	0.016 ± 0.001	1.49 ± 0.06
Epimastigotes	H-Ras-CVLL	0.016 ± 0.008	0.008 ± 0.006
	RAS-CVIM	0.014 ± 0.002	2.09 ± 0.07

PGGT-I assays were carried out by incubating the cytosol (9 μg protein) from *T. cruzi* cells (trypomastigotes or epimastigotes) at 30 °C for various time periods (0–120 min) with 0.3 μCi (0.65 μM) [<sup>3</sup>H]GGPP and 5 μM H-Ras-CVLL or RAS-CVIM. PFT assays were done by incubating the cytosol (5 μg protein) at 30 °C for various time periods (0–30 min) with 0.3 μCi (0.57 μM) [<sup>3</sup>H]FPP and 5 μM RAS-CVIM or H-Ras-CVLL. The data represent mean of the specific activity (fmol/min per μg of cytosolic protein) ± the standard deviations of two measurements for PFT and four measurements for PGGT-I.

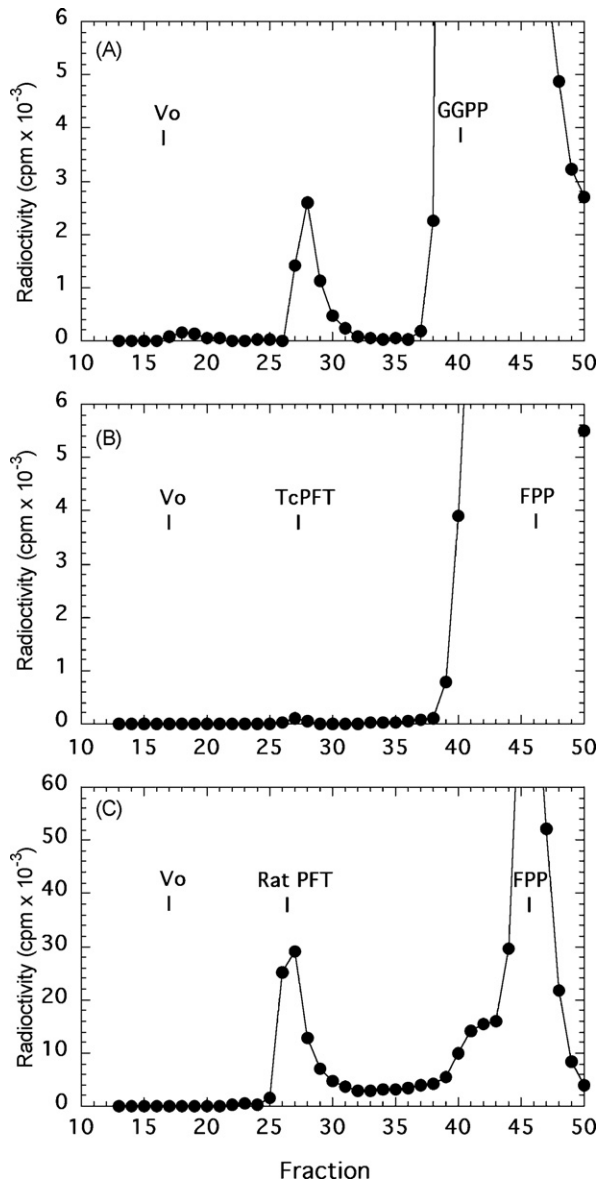


Fig. 6. Complex formation of the isolated *T. cruzi* PGGT-I with GGPP, and *T. cruzi* PFT or rat PFT with FPP. The recombinant apo-enzyme (1.5  $\mu$ g protein) of the PGGT-I or PFT was incubated with 0.5  $\mu$ Ci of [ $^3$ H]GGPP (0.54  $\mu$ M) or [ $^3$ H]FPP (0.48  $\mu$ M), respectively, and the formation of a radioactive protein complex was analyzed by chromatography on a Superdex 200 HR10/30 column. (A) A mixture of *T. cruzi* PGGT-I (partially purified by Q-Sepharose and Superdex 200 columns) and [ $^3$ H]GGPP. (B) *T. cruzi* PFT and [ $^3$ H]FPP. (C) Rat PFT and [ $^3$ H]FPP. Elution positions of the enzyme proteins, GGPP, and FPP as well as the void volume (Vo) are indicated.

mastigotes contain very low levels ( $\sim$ 0.02 fmol/min per  $\mu$ g of cytosolic protein) of [ $^3$ H]geranylgeranyl-transferring activity on H-Ras-CVLL or RAS-CVIM, which are  $\sim$ 100-fold lower than [ $^3$ H]farnesyl-transferring activity measured with RAS-CVIM. In addition, when the protein-[ $^3$ H]GGPP complex formation assays were performed with the cytosol fractions from trypomastigotes and epimastigotes, small amounts of radioactive protein were observed in Superdex 200 chromatography fractions, which contain a protein detected by Western blot with the anti-*T. cruzi* PGGT-I  $\beta$  antiserum (not shown). These suggest a

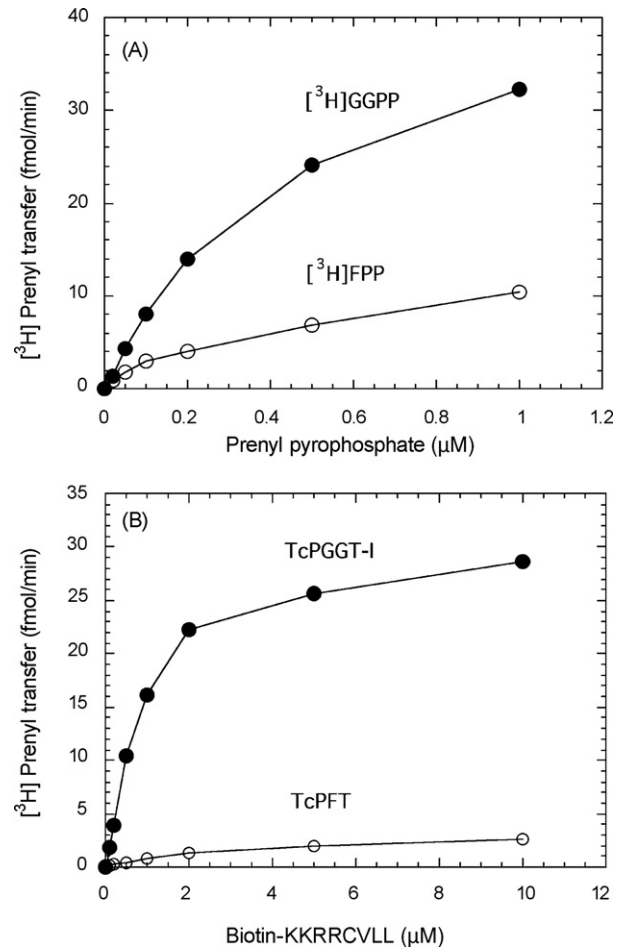


Fig. 7. C-terminal peptide KKRRCVLL of a putative *T. cruzi* Ras-like protein is selectively geranylgeranylated by *T. cruzi* PGGT-I. (A) Specificity for GGPP vs. FPP of *T. cruzi* PGGT-I to prenylate biotin-KKRRCVLL peptide. *T. cruzi* PGGT-I (partially purified, 50 ng protein) was incubated with 5  $\mu$ M biotin-KKRRCVLL and various concentrations of either [ $^3$ H]GGPP or [ $^3$ H]FPP. (B) Selective utilization of the peptide substrate by *T. cruzi* PGGT-I or PFT. Assays for geranylgeranylation by *T. cruzi* PGGT-I (partially purified, 50 ng protein) or for farnesylation by *T. cruzi* PFT (20 ng protein) were carried out with various concentrations of biotin-KKRRCVLL and 0.65  $\mu$ M [ $^3$ H]GGPP or [ $^3$ H]FPP, respectively.

low abundance of PGGT-I in both life-cycle cells of *T. cruzi*. The [ $^3$ H]geranylgeranyl-transferring activity in trypomastigotes and epimastigotes was detected with both H-Ras-CVLL and RAS-CVIM in a similar efficiency, while the [ $^3$ H]farnesyl-transferring activity in both cells shows high specificity for RAS-CVIM over H-Ras-CVLL (Table 5). These specificities are consistent with those of recombinant *T. cruzi* PGGT-I and PFT (Table 1).

### 3.9. Inhibitor studies

Several inhibitors showing high potency against mammalian PGGT-I have been developed. However, CaaX tetrapeptide mimetics containing leucine [38] and a recently developed inhibitor without a carboxylic acid [39] showed low inhibitory potency against *T. cruzi* PGGT-I at 50 nM, a concentration that caused significant inhibition of rat PGGT-I (Table 6). The CaaX mimetics GGTI-297 and FTI-276, selective inhibitors of

Table 6  
Inhibition of recombinant *T. cruzi* PGGT-I, PFT, and rat PGGT-I

Compound	% inhibition at 50 nM		
	<i>T. cruzi</i> PGGT-I	Rat PGGT-I	<i>T. cruzi</i> PFT
GGTI-297	<10	93.8 ± 5.4	92.6 ± 1.4
FTI-276	<10	64.6 ± 14.5	75.0 ± 7.4
GGTI-2154	14.7 ± 0.9	91.7 ± 4.5	13.3 ± 3.2
GGTI-2151	16.3 ± 1.8	68.7 ± 13.0	<10
GGTI-DU40	16.3 ± 3.9	95.7 ± 0.9	<10

PGGT-I inhibition assays were carried out with 50 nM of each compound using *T. cruzi* PGGT-I (50 ng) or rat PGGT-I (5 ng) and 5 μM H-Ras-CVLL as a substrate. PFT inhibition assays were done using *T. cruzi* PFT (10 ng) and 5 μM RAS-CVIM. The data represent mean ± the standard deviations of two to three measurements.

mammalian PGGT-I and PFT, respectively, had little effect on *T. cruzi* PGGT-I, whereas both of these compounds strongly inhibit *T. cruzi* PFT. Previous results show that methyl ester prodrugs of both FTI-276 and GGTI-297 inhibit growth of intracellular *T. cruzi* amastigotes more potently than they inhibit growth of mammalian host cells [21]. This may be due to inhibition of *T. cruzi* PFT by both compounds in the parasites.

Sequence identity of protozoan PFT α and β subunits from Trypanosomatids, *P. falciparum*, and *E. histolytica* is quite low (~20% identity) compared to the mammalian orthologs as well as between protozoan species. This includes a subset of the active site residues, suggesting distinct specificity of binding to CaaX peptide substrates and inhibitors between PFT enzymes from these different species [15,16,18,40]. PGGT-I β orthologs have not been identified in gene databases of *T. brucei* and *Leishmania* species. In gene databases of *Plasmodium* species, in addition to PFT β subunit, two putative proteins with 16–20% sequence identity to the family of prenyltransferase β-subunits were found (not shown), although these have not been characterized. Among protozoan organisms, PGGT-I β orthologs have been so far identified only in *T. cruzi* and *E. histolytica*, which show about 20–30% sequence identity to the orthologs from other species (Fig. 1) [19]. Phylogenetic analysis of PGGT-I β from 15 species, PFT β from 14 species, and PGGT-II β from 11 species suggests that the *T. cruzi* protein is a member of PGGT-I β family although it diverges earlier than other species PGGT-I β orthologs (not shown). Structural studies of rat PGGT-I complexed with a non-productive GGPP analog and various CaaX peptides have revealed residues that directly contact the CaaX peptide [3,9]. Of those, several residues that contact the X and/or a<sub>2</sub> residues of the Ca<sub>1</sub>a<sub>2</sub>X peptide, Thr49, His121, Ala123, and Leu320 of rat PGGT-I β, are altered to Ile, Thr, Ser, and Val, respectively, in *T. cruzi* PGGT-I β (Fig. 1), and Tyr166 of rat PGGT-I α is altered to Phe in *T. cruzi* PGGT-I. Structure modeling of the CaaX binding site of *T. cruzi* PGGT-I was performed based on the ternary complex structures of rat PGGT-I with the C-terminal peptide of TC21 KKSKTKCVIF (Protein Data Bank ID 1TNB) or the peptide KKKSSTKCVIL (1N4Q). The results show that bulkier side chains of the Ile and Ser residues of *T. cruzi* PGGT-I β versus the corresponding Thr49 and Ala123 of the rat enzyme appear to cause steric clash with the C-terminal Phe of the CVIF peptide ligand,

while the amino acid replacements seem to provide enough space to accommodate the CVIL peptide (not shown). These are consistent with the CaaX specificity of the *T. cruzi* PGGT-I (Table 1). Alterations in the residues involving substrate interactions in PFT and PGGT-I subunits between protozoan and mammalian orthologs may cause substantial differences in binding specificity for the CaaX motif and small-molecule inhibitors in protozoa and mammalian cells [15–21,40]. This suggests not only different selectivity of inhibitors against parasite PFT and PGGT-I from that of mammalian enzymes but also differential consequences of inhibitory effects of PGGT-I or PFT on cellular events in the parasites from those in mammalian cells.

*T. cruzi* PGGT-I did not show significant activity on tested protein and peptide substrates containing aromatic amino acids within the CaaX or at the X position (Tables 1 and 3). This coincides with insensitivity of *T. cruzi* PGGT-I to the CaaX mimetic inhibitors selective for mammalian PGGT-I, which contain an aromatic side group and were originally designed based on the structure of the CVFM peptide that is an inhibitor but not a substrate of mammalian PFT [41]. These results may provide useful information to design specific inhibitors against the parasite PGGT-I.

Only a few prenylated proteins have been identified so far in protozoan parasites. In the *T. cruzi* gene database, several putative proteins were found to contain the C-terminal CaaX prenylation signal motif. Among five GTPase-like proteins found to have the CaaX motif, two of those contain the C-terminal Leu (Table 2) that are predicted to be *T. cruzi* PGGT-I substrates. One putative Rab GTPase with CWLM [37] may be a PGGT-II substrate, and other two GTPase-like proteins (TcRho1-CQLF [26] and one with CHF M) seem to serve as selective *T. cruzi* PFT substrates (Table 3). Four of the *T. cruzi* PRL protein tyrosine phosphatase homologs and five of the DNAJ homologs were found to have the CaaX ending with Met and Gln (Table 2), respectively, and thus these are predicted to be farnesylated (Table 3).

Our data so far indicate that PFT inhibitors are unable to completely kill *T. cruzi* at concentrations that are below the toxic range to host cells. Based on following facts, we speculate the potential of the PGGT-I to be utilized as a drug target against *T. cruzi*. (1) It is likely that the substrate Ras-like GTPase plays essential roles in *T. cruzi* cells based on analogy to the function of mammalian Ras. (2) *T. cruzi* PGGT-I acts on the C-terminal peptide of the Ras-like GTPase as a selective substrate. (Tables 3 and 4, Fig. 7B). (3) Distinct CaaX substrate specificity and inhibitor selectivity of *T. cruzi* PGGT-I from those of mammalian enzyme (Tables 1 and 6) suggest the potential to develop selective inhibitors against this enzyme. (4) *T. cruzi* cells seem to have a low abundance of PGGT-I and a small number of its substrates (Tables 2, 3 and 5). (5) *T. cruzi* cells showed relatively low sensitivity to PFT inhibitors compared to *P. falciparum* and *T. brucei* that do not seem to have PGGT-I. A potent and specific inhibitor against *T. cruzi* PGGT-I with high cell permeability will allow us to assess if PGGT-I inhibition alone or in combination with PFT inhibition will serve as an effective treatment strategy against *T. cruzi* infection.

## Acknowledgement

This research was supported by National Institutes of Health grant AI054384.

## References

- [1] Glomset JA, Gelb MH, Farnsworth CC. Prenyl proteins in eukaryotic cells: a new type of membrane anchor. *Trends Biochem Sci* 1990;15:139–42.
- [2] Zhang FL, Casey PJ. Protein prenylation: molecular mechanisms and functional consequences. *Annu Rev Biochem* 1996;65:241–69.
- [3] Reid TS, Terry KL, Casey PJ, Beese LS. Crystallographic analysis of CaaX prenyltransferases complexed with substrates defines rules of protein substrate selectivity. *J Mol Biol* 2004;343:417–33.
- [4] Basso AD, Kirschmeier P, Bishop WR. Lipid posttranslational modifications. Farnesyl transferase inhibitors. *J Lipid Res* 2006;47:15–31.
- [5] Pompliano DL, Schaber MD, Mosser SD, Omer CA, Shafer JA, Gibbs JB. Isoprenoid diphosphate utilization by recombinant human farnesyl:protein transferase: interactive binding between substrates and a preferred kinetic pathway. *Biochemistry* 1993;32:8341–7.
- [6] Yokoyama K, McGeady P, Gelb MH. Mammalian protein geranylgeranyltransferase-I: substrate specificity, kinetic mechanism, metal requirements, and affinity labeling. *Biochemistry* 1995;34:1344–54.
- [7] Reiss Y, Brown MS, Goldstein JL. Divalent cation and prenyl pyrophosphate specificities of the protein farnesyltransferase from rat brain, a zinc metalloenzyme. *J Biol Chem* 1992;267:6403–8.
- [8] Yokoyama K, Zimmerman K, Scholten J, Gelb MH. Differential prenyl pyrophosphate binding to mammalian protein geranylgeranyltransferase-I and protein farnesyltransferase and its consequence on the specificity of protein prenylation. *J Biol Chem* 1997;272:3944–52.
- [9] Taylor JS, Reid TS, Terry KL, Casey PJ, Beese LS. Structure of mammalian protein geranylgeranyltransferase type-I. *EMBO J* 2003;22:5963–74.
- [10] Lane KT, Beese LS. Thematic review series: lipid posttranslational modifications. Structural biology of protein farnesyltransferase and geranylgeranyltransferase type I. *J Lipid Res* 2006;47:681–99.
- [11] Leung KF, Baron R, Seabra MC. Thematic review series: lipid posttranslational modifications. geranylgeranylation of Rab GTPases. *J Lipid Res* 2006;47:467–75.
- [12] Wilson AL, Erdman RA, Castellano F, Maltese WA. Prenylation of Rab8 GTPase by type I and type II geranylgeranyl transferases. *Biochem J* 1998;333:497–504.
- [13] Leung KF, Baron R, Ali BR, Magee AI, Seabra MC. Rab GTPases containing a CAAX motif are processed post-geranylgeranylation by proteolysis and methylation. *J Biol Chem* 2007;282:1487–97.
- [14] Young SG, Ambroziak P, Kim E, Clarke S. Postisoprenylation protein processing: CXXX (CaaX) endoproteases and isoprenylcysteine carboxyl methyltransferase. In: Tamanoi F, Sigman DS, editors. *The Enzymes*, XXI. San Diego: Academic Press; 2001. p. 155–213.
- [15] Buckner FS, Yokoyama K, Nguyen LN, et al. Cloning, heterologous expression, and distinct substrate specificity of protein farnesyltransferase from *Trypanosoma brucei*. *J Biol Chem* 2000;275:21870–6.
- [16] Buckner FS, Eastman R, Speelman E, et al. Cloning, heterologous expression, and substrate specificity of protein farnesyltransferases from *Trypanosoma cruzi* and *Leishmania major*. *Mol Biochem Parasitol* 2002;122:181–8.
- [17] Chakrabarti D, Da Silva T, Barger J, et al. Protein farnesyltransferase and protein prenylation in *Plasmodium falciparum*. *J Biol Chem* 2002;277:42066–73.
- [18] Kumagai M, Makioka A, Takeuchi T, Nozaki T. Molecular cloning and characterization of a protein farnesyltransferase from the enteric protozoan parasite *Entamoeba histolytica*. *J Biol Chem* 2004;279:2316–23.
- [19] Makioka A, Kumagai M, Takeuchi T, Nozaki T. Characterization of protein geranylgeranyltransferase I from the enteric protist *Entamoeba histolytica*. *Mol Biochem Parasitol* 2006;145:216–25.
- [20] Yokoyama K, Trobridge P, Buckner FS, et al. The effects of protein farnesyltransferase inhibitors on trypanosomatids: inhibition of protein farnesylation and cell growth. *Mol Biochem Parasitol* 1998;94:87–97.
- [21] Yokoyama K, Trobridge P, Buckner FS, Van Voorhis WC, Stuart KD, Gelb MH. Protein farnesyltransferase from *Trypanosoma brucei*. A heterodimer of 61- and 65-kDa subunits as a new target for antiparasite therapeutics. *J Biol Chem* 1998;273:26497–505.
- [22] Carrico D, Ohkanda J, Kendrick H, et al. In vitro and in vivo anti-malarial activity of peptidomimetic protein farnesyltransferase inhibitors with improved membrane permeability. *Bioorg Med Chem* 2004;12:6517–26.
- [23] Buckner FS, Eastman RT, Yokoyama K, Gelb MH, Van Voorhis WC. Protein farnesyl transferase inhibitors for the treatment of malaria and African trypanosomiasis. *Curr Opin Investig Drugs* 2005;6:791–7.
- [24] Gelb MH, Van Voorhis WC, Buckner FS, et al. Protein farnesyl and *N*-myristoyl transferases: piggy-back medicinal chemistry targets for the development of antitrypanosomatid and antimalarial therapeutics. *Mol Biochem Parasitol* 2003;126:155–63.
- [25] Nallan L, Bauer KD, Bendale P, et al. Protein farnesyltransferase inhibitors exhibit potent antimalarial activity. *J Med Chem* 2005;48:3704–13.
- [26] Nepomuceno-Silva JL, Yokoyama K, de Mello LD, et al. TcRho1, a farnesylated Rho family homologue from *Trypanosoma cruzi*: cloning, trans-splicing, and prenylation studies. *J Biol Chem* 2001;276:29711–8.
- [27] Cuevas IC, Rohloff P, Sanchez DO, Docampo R. Characterization of farnesylated protein tyrosine phosphatase TcPRL-1 from *Trypanosoma cruzi*. *Eukaryot Cell* 2005;4:1550–61.
- [28] Hertz-Fowler C, Peacock CS, Wood V, et al. GeneDB: a resource for prokaryotic and eukaryotic organisms. *Nucleic Acids Res* 2004;32(Database issue):D339–43.
- [29] Weston D, Patel B, Van Voorhis WC. Virulence in *Trypanosoma cruzi* infection correlates with the expression of a distinct family of sialidase superfamily genes. *Mol Biochem Parasitol* 1999;98:105–16.
- [30] Van Voorhis WC, Eisen H. Fl-160. A surface antigen of *Trypanosoma cruzi* that mimics mammalian nervous tissue. *J Exp Med* 1989;169:641–52.
- [31] Siegel TN, Tan KS, Cross GA. Systematic study of sequence motifs for RNA trans splicing in *Trypanosoma brucei*. *Mol Cell Biol* 2005;25:9586–94.
- [32] Terry KL, Casey PJ, Beese LS. Conversion of protein farnesyltransferase to a geranylgeranyltransferase. *Biochemistry* 2006;45:9746–55.
- [33] Ye M, Shima F, Muraoka S, et al. Crystal structure of M-Ras reveals a GTP-bound “off” state conformation of Ras family small GTPases. *J Biol Chem* 2005;280:31267–75.
- [34] Bourne HR, Sanders DA, McCormick F. The GTPase superfamily: conserved structure and molecular mechanism. *Nature* 1991;349:117–27.
- [35] Diamond RH, Cressman DE, Laz TM, Abrams CS, Taub R. PRL-1, a unique nuclear protein tyrosine phosphatase, affects cell growth. *Mol Cell Biol* 1994;14:3752–62.
- [36] Tibbetts RS, Jensen JL, Olson CL, Wang FD, Engman DM. The DnaJ family of protein chaperones in *Trypanosoma cruzi*. *Mol Biochem Parasitol* 1998;91:319–26.
- [37] El-Sayed NM, Myler PJ, Bartholomeu DC, et al. The genome sequence of *Trypanosoma cruzi*, etiologic agent of Chagas disease. *Science* 2005;309:409–15.
- [38] Vasudevan A, Qian Y, Vogt A, et al. Potent, highly selective, and non-thiol inhibitors of protein geranylgeranyltransferase-I. *J Med Chem* 1999;42:1333–40.
- [39] Peterson YK, Kelly P, Weinbaum CA, Casey PJ. A novel protein geranylgeranyltransferase-I inhibitor with high potency, selectivity, and cellular activity. *J Biol Chem* 2006;281:12445–50.
- [40] Eastman RT, White J, Huckle O, et al. Resistance to a protein farnesyltransferase inhibitor in *Plasmodium falciparum*. *J Biol Chem* 2005;280:13554–9.
- [41] Reiss Y, Goldstein JL, Seabra MC, Casey PJ, Brown MS. Inhibition of purified p21ras farnesyl:protein transferase by Cys-AAX tetrapeptides. *Cell* 1990;62:81–8.